



# Parameters of cold pilgering of seamless steel tube

Zhi-bing Chu<sup>1,2</sup> · Zhan-yuan Xue<sup>2</sup> · Duo Zhang<sup>2</sup> · Huan-zhu Wang<sup>2</sup> · Wei Li<sup>2</sup> · Ren-huai Liu<sup>1</sup> · Qing-xue Huang<sup>2</sup>

Received: 28 February 2018 / Revised: 24 October 2018 / Accepted: 29 October 2018 / Published online: 30 April 2019  
© China Iron and Steel Research Institute Group 2019

## Abstract

As the process parameters of pilger cold-rolled seamless steel tubes are basically based on experience leading to the generation of defects, 304 stainless steel was chosen and the important process parameters including the feed, rotation angle and  $Q$  value (the ratio of the length of the deformation section to that of the finishing section) were selected to analyze the effect of different process parameters on the tube forming process and rules. The results show that during the cold rolling process, the rolling force, the equivalent stress of the tube, the residual stress and the springback of the external diameter increased with the increase in the feed rate and the rotation angle and the decrease in  $Q$  value. Increasing the feed quantity and decreasing  $Q$  value will lead to the decrement in the roundness of the pipe. After comprehensive evaluation of the advantages and disadvantages, a set of optimal parameters are selected to carry out the experiment. The residual stress and the outer diameter of the finished products were measured. The results of the measurement and the numerical simulation results are within reasonable range, and the accuracy of the numerical simulations and the influence of the process parameters on the pilger cold rolling are further verified.

**Keywords** Cold rolling · Process parameter · Numerical simulation · Residual stress · Springback · Rolling force

## 1 Introduction

Pilger cold rolling is an important technology of rolling metal pipe and it has been widely used in processing titanium, zirconium alloy and other metal pipe manufacturing, whose accumulated deformation section is large [1–6]. Later, Ukai et al. [7] proposed pilger cold rolling technology which can also be used to process low-plasticity metal such as oxide dispersion strengthened metal. The cold pilger rolling process is a complicated plastic forming process of reducing diameter and wall, due to its deformation characteristics and complex geometry. At an early stage, scholars [8–10] only used finite element method to qualitatively study the pilger cold rolling process. With the

improvement in technical means, the researches on pilger cold rolling were further deepened. Montmitonnet et al. [11] carried out a theoretical study on the inner surface lubrication condition of pilger cold-rolled zirconium alloy pipe. Abe et al. [12] proposed a new lubrication calculation method using the Reynolds equation. Pociecha et al. [13] proposed a new pilger cold rolling technique and analyzed the deformation process. However, the domestic researches on pilger cold rolling mainly focus on the pass design [14, 15].

In the actual production, the design about process parameters of different metals is based on the production experience. If improper process parameters are selected, the possibility of defects such as lateral indentation and longitudinal burrs will be greatly increased. Therefore, a reasonable design of process parameters is critical. Few scholars have studied the process parameters of the cold rolling process. Abe and Furugen [16] analyzed the deformation behavior of pilger rolling and obtained the suitable rolling process conditions to ensure the surface quality of the finished pipe. Randall and Prieur [17] along with Abe et al. [18] analyzed the influence of process parameters on pipe accuracy in the pilger cold rolling

✉ Zhi-bing Chu  
chuzhibing@tyust.edu.cn

<sup>1</sup> School of Mechanics and Civil Engineering, Jinan University, Guangzhou 510632, Guangdong, China

<sup>2</sup> Heavy Machinery Engineering Research Center of Ministry of Education, Taiyuan University of Science and Technology, Taiyuan 030024, Shanxi, China

process. In the domestic, three-roll cold rolling process parameters on the quality of finished products were studied [19]. Liu et al. [20] studied the influence of cold rolling parameters on the metal flow and forming load of TA18 titanium alloy tube by finite element simulation, where the rolling process is not systematic studied because the pipe deformation zone is prefabricated.

304 stainless steel and common parameters of cold rolling process used in actual production were selected to analyze the rule that different process parameters influence the tube forming process and mechanical product size through systematic numerical simulations of the pilger cold rolling process under different process parameters. Combined with the rolling experiments, the simulation results were verified, which can be used for the process control of pilger cold-rolled steel pipe in the actual production.

## 2 Pilger cold rolling process

Figure 1 shows a schematic diagram of pilger cold rolling. Figure 1 shows that during the pilger cold rolling of the seamless pipe, the pipe is deformed in a closed pass consisting of roll and mandrel, which is constantly changing with the movement of the rolls. The upper and lower rolls open the pass with varying diameters on the circumferential surface of the rolling groove. The cross-sectional diameter of mandrel and roll groove is also constantly changing correspondingly. During the rolling process, the pipe and the mandrel cannot move under the restriction of the chuck. The process of the roll moving from the rear limit position to the front limit position is called the forward stroke, and the process of the roll moving from the front limit position to the rear limit position is called the

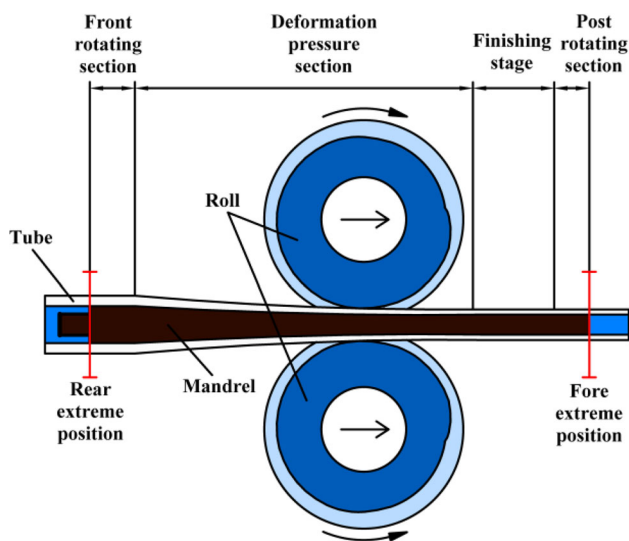


Fig. 1 Schematic view of cold pilgering

back stroke. The feeding and turning of the pipe are completed in the forward and back limit positions [21]. Pilger cold rolling process can also be divided into four different stages of the back rotary section, including the deformation pressure section, the finishing section, the front rotary section and back rotary section. The function of the front and back rotary section is achieving pipe rotary and feeding pipe, respectively. There is no deformation of the tube in this process. In the early stage of the deformation section, the main occurrence is reducing the diameter and the deformation of the wall is more obvious in the middle and late stages. Thus, the deformation can be divided into the reducing section and wall thickness reduction. The finishing section is mainly used for finishing the pipe, and the ratio of the length of the deformation section to that of the finishing section is  $Q$  value, which is the important process parameter of pilger cold rolling.

Figure 2a shows pilger cold-rolled section of the deformation characteristics, and it can be seen that the cross section of the deformed section of the pipe is not oval after the rolling. Pilger cold-rolled pipe is a continuous process of rotary feeding, die rolling and finishing the final shape. As shown in Fig. 2b, the cross section of the tube can be divided into different deformation zones, including perforated ridge zone 1, perforated side wall zones 2, 3 and perforated opening zone 4. The deformation characteristics of different deformation zones in the cold rolling process are also different. In this paper, the main research object is the rolling front stroke. In the front stroke, groove-shaped ridge zone 1 and groove-shaped sidewall zones 2 and 3 are in three-direction (axial, radial and circumferential) compressive state, and bore-type opening zone 4 is in a uniaxial (an axial) stress state.

## 3 Establishment and analysis of numerical model

### 3.1 Numerical model and craftwork plan

Figure 3 shows a three-dimensional finite element model of 304 stainless steel tube with pilger cold rolling, which includes tube, mandrel, upper/lower roll and pusher. The material parameters of 304 stainless steel can be read from the material library of DEFORM-3D. According to actual rolling that the roll, mandrel and pusher are all high-alloy steel, simulation is set as a rigid body, the tube is an elastoplastic body, and Coulomb friction is used between all contact pairs in the whole rolling process. The Coulomb friction coefficient is 0.1. The complex roll motion in actual production is simplified to reciprocate translational and rotational motion. The finite element calculation follows the Prandtl–Reuss flow equation and the von Mises

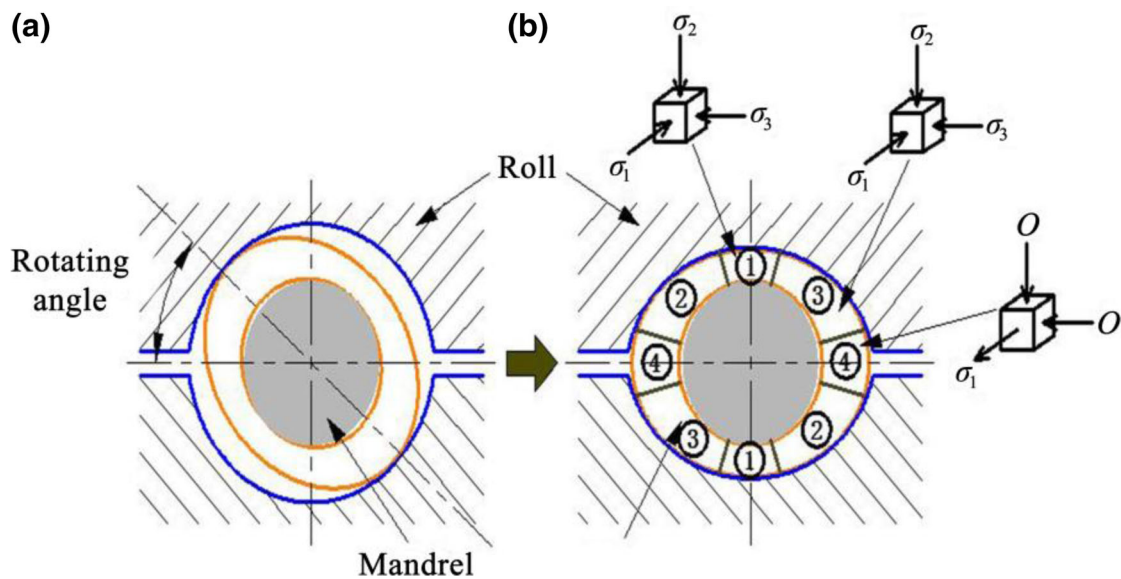


Fig. 2 Cross-sectional deformation features of during cold pilgering. **a** Cross-sectional shape after rotating; **b** distribution of rolling forming area

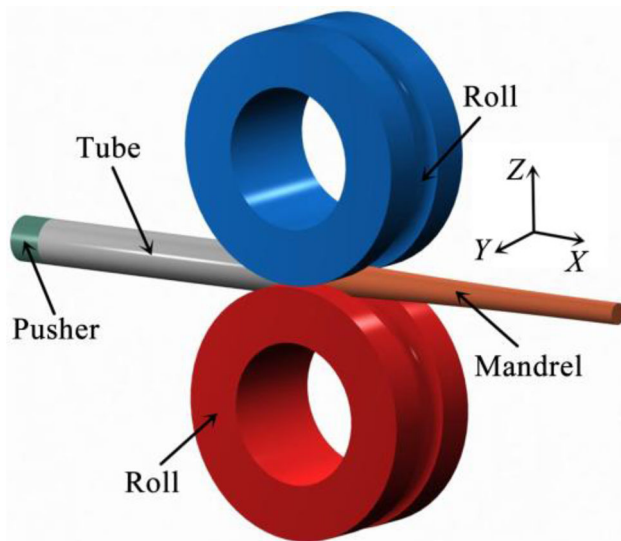


Fig. 3 Model of cold pilgering

yield criterion, and is solved by the Newton–Raphson method. The grid element type is a four-node tetrahedral element. The initial tube size is  $\phi 67 \text{ mm} \times 6 \text{ mm}$ , the finished tube size is  $\phi 38 \text{ mm} \times 3 \text{ mm}$ , and the cold rolling complete process with a cycle feed of 10 mm was simulated.

The main parameters affecting the forming process of pilger cold rolling include feed value ( $m$ ), rotation angle ( $\theta$ ) and  $Q$  value. In this paper, several parameters are selected according to experience in actual production as shown in Table 1. Through the post-processing module, the rolling force, equivalent stress, springback and residual stress in rolling process were compared, and the influence rule of

Table 1 Rolling parameters used in this study

No.	$m/\text{mm}$	$\theta/(\text{°})$	$Q$ value
1	8	50	4.0
2	10	60	4.4
3	12	70	–

process parameters on cold rolling forming was analyzed. Without affecting the accuracy of the results, in order to improve the work efficiency, the rotation angle and  $Q$  value are fixed at  $60^\circ$  and 4.4, respectively, when the influence rule of different feed volumes is analyzed. When analyzing the influence rule of different turning angles on forming, the feed value and  $Q$  value are fixed at 10 mm and 4.4, respectively. When analyzing the influence of  $Q$  value on the shaping, the feed value amount and the rotation angle are fixed at 10 mm and  $60^\circ$ , respectively.

## 3.2 Numerical simulation results and analysis

### 3.2.1 Effect of different process parameters on rolling force

Figure 4 shows the rolling force changing curves of different process parameters. Figure 4a shows that when the feed value increases, the rolling force increases significantly. The difference of maximum rolling force under different delivery amounts is up to more than  $10^5 \text{ N}$ . Figure 4b shows that the rolling force increases to a certain extent with the increase in the rotation angle, but the increase caused by the increase in the feed value is more significant. The rolling force variation curve in Fig. 4c

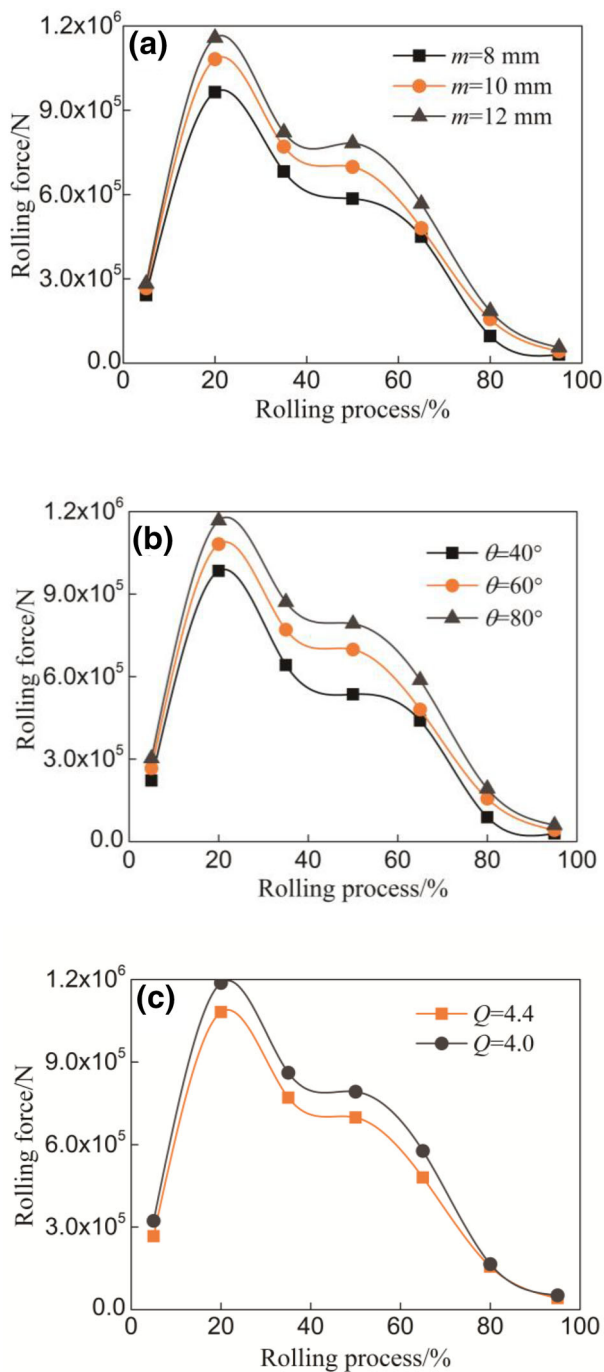


**Fig. 4** Curves of rolling force changing with different feed values (a), rotation angles (b) and  $Q$  values (c)

should be compared with that in Fig. 4a. When  $Q$  value decreases, the rolling force also increases obviously. When the feed value is 10 mm and  $Q$  value is 4 under same rotation angle, the rolling force reaches  $1.2 \times 10^6$  N, which is more than  $5 \times 10^4$  N when  $Q$  value is 4.4 and the feed value is 12 mm. The above rules can draw a conclusion that rolling force in cold rolling process increases with

increasing feed value and the rotation angle, and decreases with the increase in  $Q$  value. There are two reasons: The first is that the increase in feed value and the reduction in  $Q$  value are equivalent to increase the deformation of each deformation section, which leads to the strong deformation of the metal and the increase in the rolling force, and the second reason is that the cross section of the pipe is oval after rolling. Increasing the rotation angle indirectly increases the deformation, which leads to roll force increasing.

### 3.2.2 Effect of different process parameters on equivalent stress

Figure 5 shows the maximum equivalent stress curves with different process parameters. Figure 5 shows that the maximum equivalent stress on the deformation section of the pipe increases with the increase in the feed value and rotation angle, and the decrease in  $Q$  value in the rolling process. During the rolling process, the increase in feed value and rotation angle as well as the decrease in  $Q$  value leads to the increase in the deformation of the pipe section, which leads to the increase in the maximum equivalent stress. In the initial stage of rolling, the maximum equivalent stress of the pipe deformation section is basically the same under different feed values and rotation angles, while the maximum equivalent stress under different  $Q$  values is somewhat different. This is because at the initial stage of rolling, the pipe deformation section is non-rolling pipe. The change in the feed value and the rotation angle will not cause the variation in the pipe deformation, but the decrease in  $Q$  value will lead to the increase in the deformation amount during the deformation phase, which leads to effective stress increasing. During the whole rolling process, the maximum equivalent stress when  $Q$  value changes to 4 under the same process parameters is greater than that with the increase in the feed value to 12 mm and the angle of rotation to  $80^\circ$ .

Figure 6 shows the ratio between the maximum equivalent stresses in the sidewall area of the pass and the ridge area during the different deformation stages of the rolling process. It can be seen that the equivalent stress values in different areas of the pipe circumference are not the same, and during the rolling processing, the ratio increases first and then decreases. The maximum equivalent stress ratio increases with the increase in the feed value and the decrease in  $Q$  value, which causes the heterogeneity of pipe circumference deformation. As the  $Q$  value increases, the ratio decreases with the increase in rotation angle, and it shows that increasing the rotation angle is conducive to pipe circumference uniform deformation.



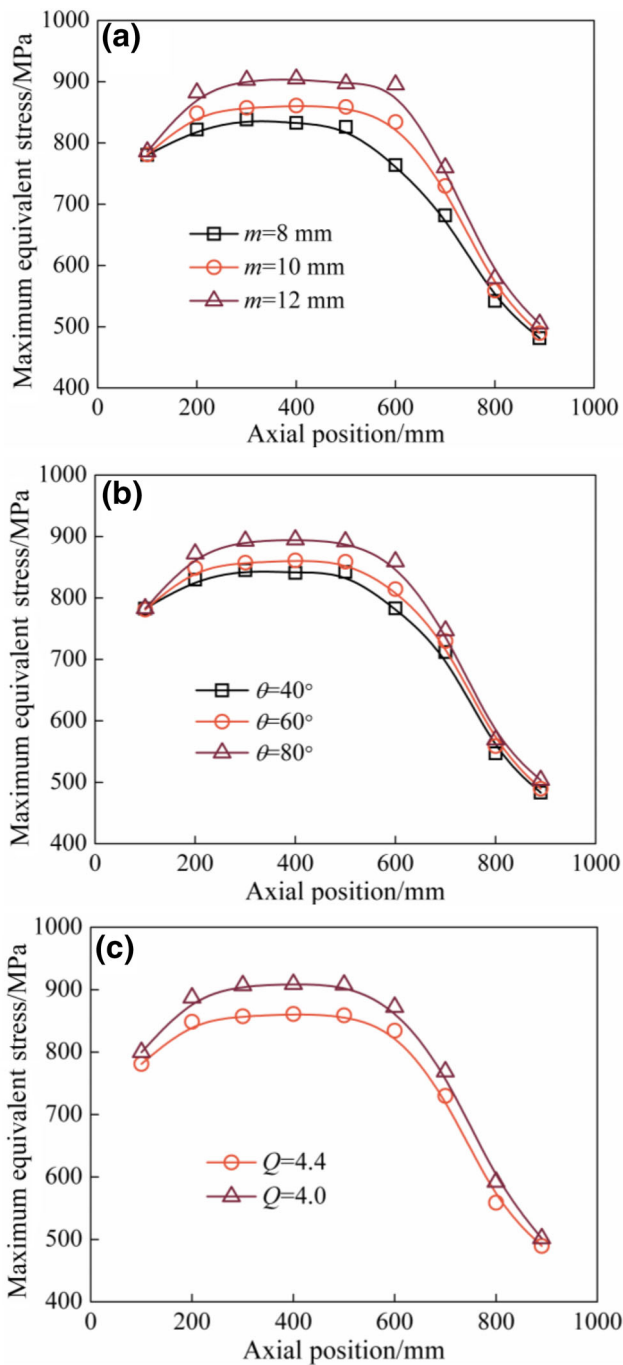


**Fig. 5** Curves of maximum equivalent stress with different feed values (a), rotation angles (b) and  $Q$  values (c)

### 3.2.3 Effect of different process parameters on residual stress

Figure 7 shows the average residual stress curve with different process parameters. It can be seen that the average residual stress of the pipe during the initial rolling is the largest and then decreases with the rolling. This is because during the initial rolling, large deformation and uneven

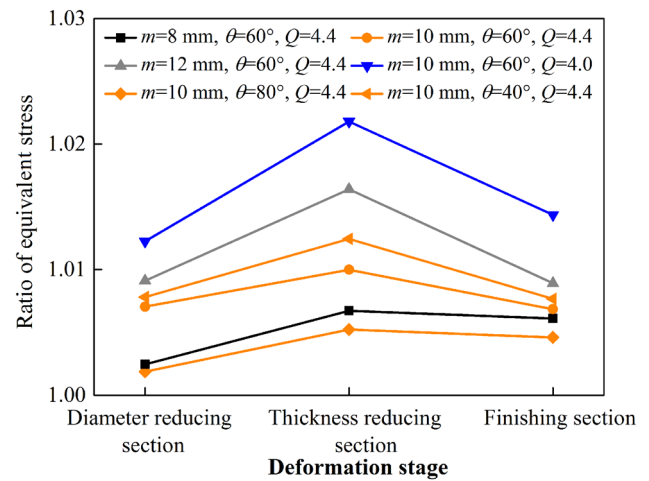


**Fig. 6** Variation in ratio between maximum equivalent stresses with different regions in different deformation stages. A Diameter reducing section; B thickness reducing section; C finishing section

deformation of the pipe lead to large residual stress; however, the residual stress decreases with the change in the stress state of the pipe after multiple cycles of rolling and finishing as well as the phase change in the pipe metal. Figure 7a shows that the average residual stress of the deformed section increases with the increase in feed value, and the larger the feeding amount, the larger the increase in residual stress is. As shown in Fig. 7b, the average residual stress increases with the rotation angle, but the increase is insignificant. This is because increasing the rotation angle increases the deformation at the side wall of the pass section of the pipe, but increasing the rotation angle makes pipe circumference deformation more uniform. Figure 7c shows that the average residual stress increases with the decrease in  $Q$  value, and the residual stress at  $Q = 4.0$  is obviously higher than that at  $Q = 4.4$ .

Figure 8 shows the ratio between the residual stresses in the sidewall area of the pass and the ridge area during the different deformation stages of the rolling process. It can be seen from that as the rolling processes, the ratio first increases and then decreases; at the same time, it also shows that there is some difference between the residual stress values in different deformation zones of pipe circumference. The ratio between the residual stresses which decreases with the increase in the rotation angle increases with the increase in feed value and the decrease in  $Q$  value.

### 3.2.4 Effect of different process parameters on springback

To study the influence rule of the process parameters on the pilger cold rolling rebound, the pipe sections were intercepted separately into the four stages of springback section, wall thickness reduction section, finishing section and finished product. Table 2 shows comparison of each point on

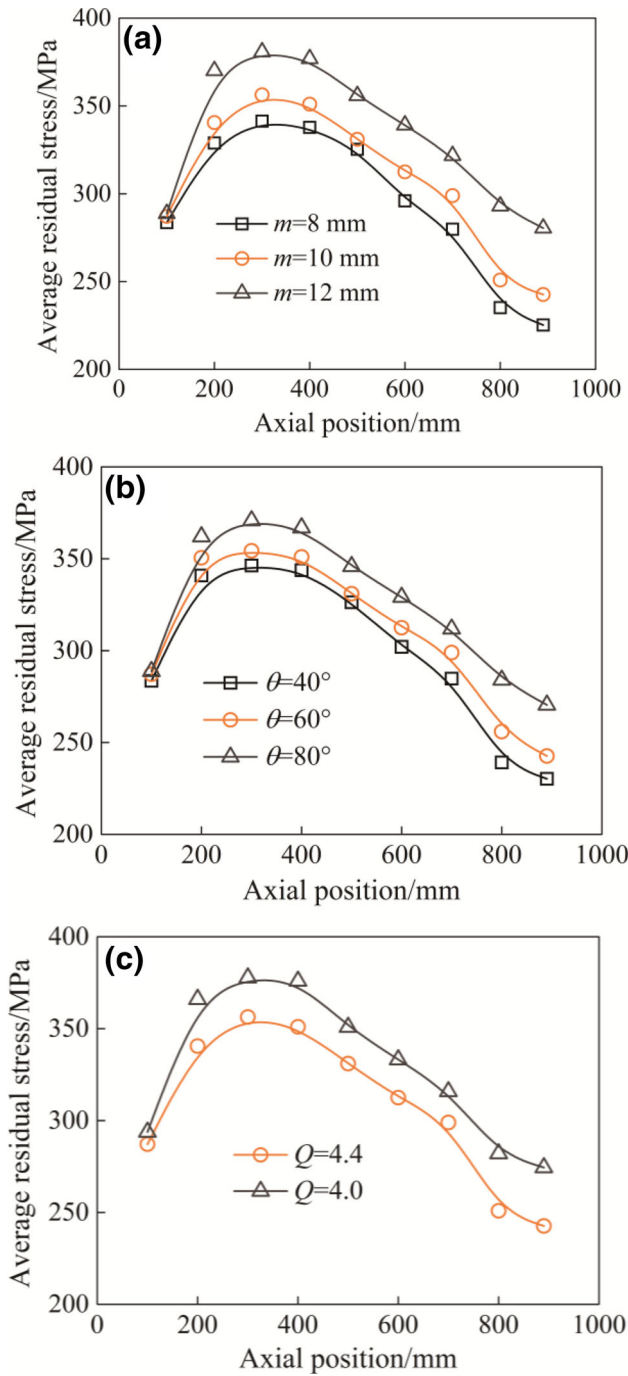


Fig. 7 Curves of average residual stress with different feed values (a), rotation angles (b) and  $Q$  values (c)

the cross section of the pipe section of the springback deformation under different process parameters. Table 1 shows that the springback value at each point of cross section of pipe increases with the increase in feed value and rotation angle, and the decrease in  $Q$  value. This is because the amount of deformation and pipe stress increases when the above process parameters change. It can also be seen that when the feed value and  $Q$  value

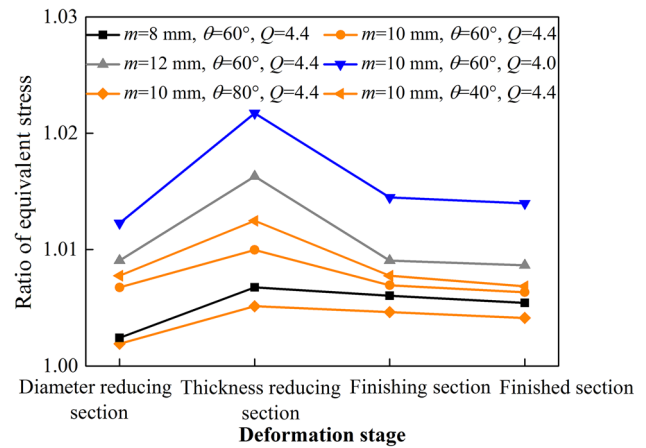


Fig. 8 Ratio between maximum residual stresses of different regions in different deformation stages.  $D$  Finished section

increase, the difference in the springback of each point on the pipe cross-sectional deformation increases, which also causes uneven deformation of the cross section and the decline of the pipe roundness. On the contrary, when the rotation angle increases, the difference in the springback of each point on the pipe cross-sectional deformation decreases. This is because when the rotation angle increases, the difference of radial compressive stress in different deformed areas of the cross section in the pipe decreases, which leads to a more even deformation of the pipe section.

### 4 Discussion

The relationship between residual stress and springback of finished product pipe is obtained by intercepting the residual stress and springback of any point in the finished pipe under different process parameters. Figure 9 shows the relationship between residual stress and rebound of finished pipe. It can be seen that the increase in springback on finished pipe is almost proportional to the increase in residual stress. Therefore, considering the influence of the above process parameters on the pilger cold forming and the simulation data, it can be concluded that increasing the feed value, the rotation angle and decreasing  $Q$  value will cause the increase in the rolling force. However, during the rolling process, the increase in the rolling force will accelerate the roll wear and put forward higher requirements on the driving equipment. From the law of the effect of equivalent stress, it can be seen that under different process parameters, the equivalent stress of the pipe in the entire deformation section is above 400 MPa; that is to say, the above process parameters can lead to plastic deformation of pipe material. However, when the feed value increases to 12 mm, the rotation angle increases to 80°,

**Table 2** Contrast of springback on each cross section with different parameters

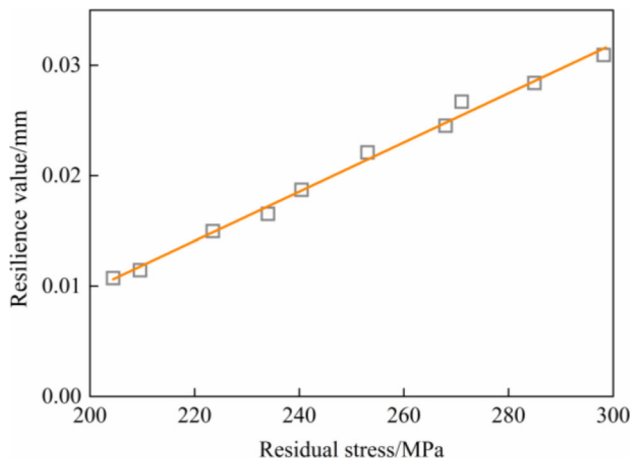
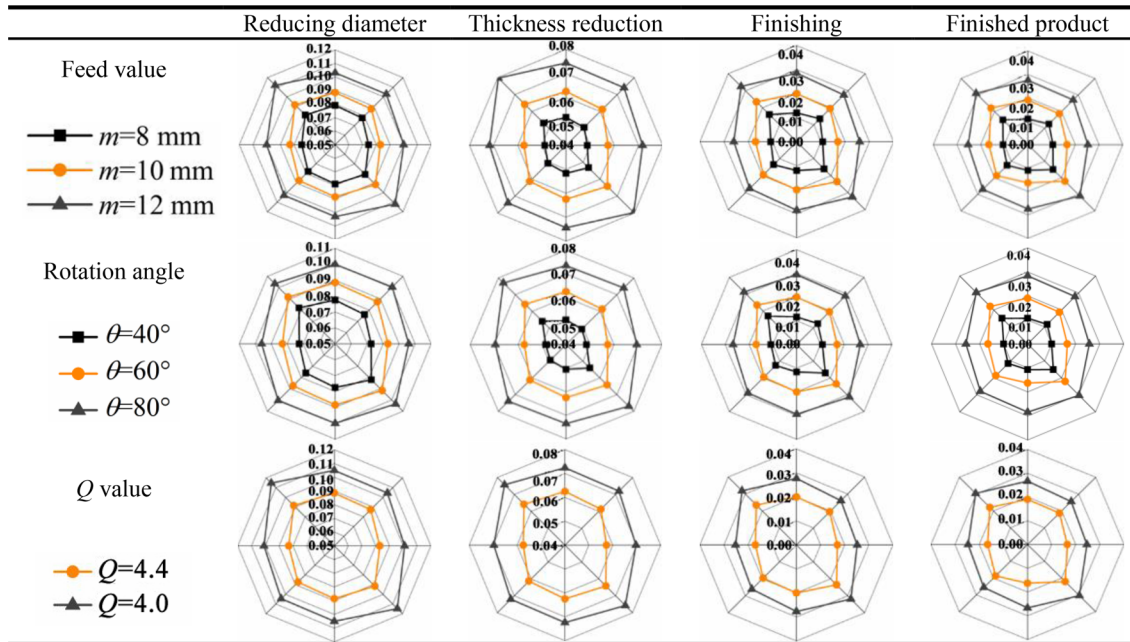


**Fig. 9** Relationship between residual stress and springback of finished tube

$Q$  value becomes 4.0, and the maximum equivalent stress of the pipe in the middle stage of the deformation section exceeds 900 MPa, which also surpasses extreme strength of 304 stainless steel, and is most likely to form cracks or other defects during rolling. The residual stress in the rolling process is one of the important indicators to measure the performance of the pipe. The difference of average residual stress of the pipe with feed values of 10 and 8 mm is not very significant, but when the feed value increases to 12 mm and  $Q$  value becomes 4.0, the average pipe residual stress has a significant increase, which will adversely affect



**Fig. 10** Finished tube after rolling

pipe performance. For the specifications of the pipe used in this paper, the maximum diameter of the pipe springback used in industry cannot exceed 0.04 mm. When the feed value increases to 12 mm and  $Q$  value becomes 4.0, the finished pipe springback will be greater than the standard requirements; when the rotation angle increases to  $80^\circ$ , the pipe springback to a certain extent exceeds the accuracy requirements; and when the rotation angle is down to  $40^\circ$ , it will greatly reduce the pipe roundness. Therefore, considering rolling production efficiency and product performance factors in many aspects comprehensively, the process parameters can meet the forming requirements with the feed value of 10 mm, rotation angle of  $60^\circ$  and  $Q$  value of 4.4.

**Table 3** Contrast of experimental measurement results and numerical simulation results

Parameter	1	2	3	4	5	Experimental average data	Numerical simulation average data
Springback outer diameter/mm	0.055	0.034	0.043	0.038	0.035	0.0398	0.042
Residual stress/MPa	271.77	225.62	263.47	245.36	233.89	248.22	242.61

## 5 Experimental verification

The experiment was carried out using a LG60 mill in a stainless steel tube plant, and the finished product pipe is shown in Fig. 10. Before cold rolling, the outer diameter of the pipe is 67 mm and the wall thickness is 6 mm. After cold rolling, the theoretical outer diameter of the pipe is 38 mm, the wall thickness is 3 mm, the feed value in the process parameters is 10 mm, the rotation angle is 60°, and  $Q$  value is 4.4.

The springback outer diameter and residual stress were measured at five positions of the finished tube at random. The finished tube was subjected to wire cutting, and five sets of samples at different positions were obtained. According to the principle of residual stress measurement by X-ray diffraction, five sets of samples were measured by a laboratory Proto X-ray residual stress tester, and the measurement is shown in Table 3. Table 3 presents a comparison between the experimental measurement results and the numerical simulation results. It can be seen that the numerical simulation results of the experimental results are basically consistent, the error is within the reasonable range, and the accuracy of numerical simulation results is further verified.

## 6 Conclusions

1. By comparing the numerical simulation data of pilger cold rolling process with different process parameters, the results show that the rolling force, the maximum equivalent stress and average residual stress of pipe deformation and the springback amount of the pipe deformation section all change with the process parameters. Increasing the feed value and the rotation angle and decreasing  $Q$  value will increase the rolling force, the maximum equivalent stress of the pipe deformation section, the average residual stress and the springback; increasing the feed value and reducing  $Q$  value will lead to the decline of pipe roundness; and increasing the rotation angle will increase the pipe roundness.
2. By analyzing the optimal process parameters, the residual stress and the diameter of the finished pipe were measured and compared with the numerical simulation results. It can be concluded that the error of the two data is within a reasonable range, the accuracy of the numerical simulation is validated, and the correctness of the above influence laws is verified, which is very important and valuable to properly select the process parameters in actual production.

**Acknowledgements** The authors are grateful to the National Natural Science Foundation of China (Grant No. U1710113), the China Postdoctoral Science Foundation (Grant No. 2017M622903), the National Key Research and Development Program of Shanxi Province (Grant No. 201703D121008), the Project of Excellent Graduate Innovation in Shanxi (Grant No. 2017SY077) and the Graduate Innovation Funding Scheme for “Heavy Machinery” (Grant Nos. 20172001 and 20172004) for financial support and authorization to publish this work.

## References

- [1] D. Sornin, E.A. Pachón-Rodríguez, E. Vanegas-Márquez, K. Mocellin, R. Logé, J. Mater. Eng. Perform. 25 (2016) 4059–4069.
- [2] K.S. Raggar, S. Primig, R. Daniel, R. Kaiser, J. Paal, C. Mitterer, B. Buchmayr, Mater. Charact. 128 (2017) 257–268.
- [3] Y. Azizoğlu, M. Gärdöback, B. Sjöberg, L. Lindgren, Procedia Eng. 207 (2017) 2370–2375.
- [4] H. Stinnertz, Tube Pipe Technol. 87 (1988) 27–31.
- [5] B. Lodej, K. Niang, P. Montmitonnet, J.L. Aubin, J. Mater. Process. Technol. 177 (2006) 188–191.
- [6] J. Osika, W. Libura, J. Mater. Process. Technol. 34 (1992) 325–332.
- [7] S. Ukai, S. Mizuta, T. Yoshitake, T. Okuda, M. Fujiwara, S. Hagi, T. Kobayashi, J. Nucl. Mater. 283 (2000) 702–706.
- [8] C. Zheng, H.W. Song, S.Y. Deng, S.H. Zhang, Procedia Eng. 207 (2017) 2346–2351.
- [9] H.Q. Zhang, X.F. Wang, B.L. Wei, H. Li, Int. J. Adv. Manuf. Technol. 92 (2017) 2169–2183.
- [10] Y. Barzegar, R.J. Nedoushan, A. Razazzade, M. Farzin, D. Banabic, Proc. Romanian Acad. Ser. A 17 (2016) 267–276.
- [11] P. Montmitonnet, D. Farrugia, J.L. Aubin, F. Delamare, Wear 152 (1992) 327–342.
- [12] H. Abe, T. Nomura, Y. Kubota, J. Mater. Process. Technol. 214 (2014) 1627–1637.
- [13] D. Pocięcha, B. Boryczko, J. Osika, M. Mroczkowski, Arch. Civil Mech. Eng. 14 (2014) 376–382.



- [14] F.Y. Yan, Pass design of LG730 cold-rolling pilger mill and its finite element simulation in the rolling process, Yanshan University, Qinhuangdao, China, 2015.
- [15] X.F. Zhou, *Forg. Stamp. Technol.* 37 (2012) No. 3, 55–58.
- [16] H. Abe, M. Furugen, *J. Mater. Process. Technol.* 212 (2012) 1687–1693.
- [17] S.N. Randall, H. Prieur, *Iron Steel Eng.* 2 (1967) 109–117.
- [18] H. Abe, T. Iwamoto, Y. Yamamoto, S. Nishida, R. Komatsu, *J. Mater. Process. Technol.* 231 (2016) 277–287.
- [19] T. Fan, Research on three-roller cold rolling process of 302 stainless steel tube, Shenyang Ligong University, Shenyang, China, 2012.
- [20] J.L. Liu, W.D. Zeng, Z.L. Du, H. Tao, J.H. Xi, Y. Shu, J.Z. Yang, *Titan. Ind. Prog.* 32 (2015) 3 21–25.
- [21] L. Huang, Z. Xu, C. Dai, S. X. Hui, W.J. Ye, G. Wang, S.S. Xie, H.W. Li, *Rare Metal Mater. Eng.* 42 (2013) 524–529.